Correlation of wind and precipitation annual aggregate severity of European cyclones

Toby P. Jones, David B. Stephenson and Matthew D. K. Priestley

Department of Mathematics and Statistics, University of Exeter, UK

Introduction

Extratropical cyclones are a major cause of wind damage and flooding in mid-latitudes. While there have been several recent studies that have investigated the joint behaviour of wind and rain for *individual* extratropical cyclones (Raveh-Rubin and Wernli, 2015; Martius *et al.*, 2016; Catto and Dowdy, 2021; Owen *et al.*, 2021), fewer studies have focused on *accumulated* (aggregate) losses (Hillier and Dixon, 2020; Bloomfield *et al.*, 2023).

As well as being resilient to individual hazard events, society also needs to be able to cope with aggregate losses caused by a series of events. This is particularly so for extreme European storms, which have the propensity to occur in temporal clusters, for example, the total insured loss of €10.5 billion caused by eight storms (including *Daria*, *Vivian* and *Wiebke*) in December 1989 to January 1990 (Mailier *et al.*, 2006) and €13 billion from *Anatol*, *Lothar* and *Martin* in December 1999 (Ulbrich *et al.*, 2001). Quantification of aggregate losses and their dependencies is a key concern for the reinsurance industry (Kaas *et al.*, 2008). Despite wind and rain in storms being related, risk modellers often use separate catastrophe models to simulate independent wind and flood loss events.

If wind and rain extremes were independent, one would expect a positive correlation between aggregate wind and rain-related losses simply because more storms in a given period will lead to larger values in both wind and flood-related aggregate losses. However, wind and rain extremes in extratropical cyclones are not independent and so this study explores the following questions:

- What is the correlation between the aggregate severity of wind and precipitation over Europe and the N. Atlantic regions?
- How does this correlation depend on the choice of intensity thresholds used to define wind- and precipitation-related severe losses?

Extratropical cyclones can be classified as multivariate compound events (Zscheischler *et al.*, 2020) as their impact comes from two hazards: extreme wind and precipitation. This study provides another method to explore the relationship between hazards from multivariate compound events, adding to the limited tools available (Bevacqua *et al.*, 2021). When considering aggregated impact, cyclones occurring in clusters allow them to also be classed as temporal compound events. It is feasible to expand the methods used in this study to other multivariate compound events or temporally compounding events (as defined in Zscheischler *et al.* (2020)).

Aggregate severity

This section describes what is meant by aggregate severity and how it can be quantified with an *Aggregate Severity Index* (*ASI*) (Box 1). It also briefly reviews previous studies of aggregate severity of European storms.

Equation 1 uses a threshold (u_X) to categorise damage. This function assumes damage only occurs when the value of the given meteorological variable exceeds u_X. For wind gust speeds the threshold $u_X = 20\text{ms}^{-1}$ is often used, however Klawa and Ulbrich (2003) note this threshold may be

Box 1. Definition of Aggregate Severity Index (ASI)

Suppose that N storms impact a given location over a specified time period, and let $\{X_1, X_2, \ldots, X_N\}$ be the values of a meteorological hazard variable (e.g. maximum wind gust speed) recorded for these events in a given time period. We assume that the severity (damage) at this location can be represented as a non-negative monotonically non-decreasing function of the local hazard variable. Such functions are often designed to be well correlated with insured losses.

For example, Klawa and Ulbrich (2003), and many subsequent studies, have represented wind storm severity using the conceptual loss function of form

$$g(X) = \begin{cases} (X - u_X)^k & X > u_X \\ 0 & X \le u_X. \end{cases} \quad (1)$$

with $k=3$ and where threshold u_X is chosen to be high (e.g. 20ms^{-1} or a local high percentile of near surface instantaneous wind gusts). An even simpler severity function capturing the key essential features is to use $k=1$, the excess $X - u_X$ above threshold u_X if $X > u_X$. This simpler index will be used in this paper as it has the advantage that it gives statistics that are less influenced by outlier extreme events in X.

The total damage caused by the set of N storms can be quantified using the Aggregate Severity Index (ASI) defined by the random sum

$$S_X = g(X_1) + g(X_2) + \ldots + g(X_N). \quad (2)$$

As this study uses gridded meteorological data, Equations 1 and 2 will be used to calculate an ASI at each grid point. Following typical annual contract periods used for windstorm insurance, the ASIs are calculated over the period 1 January to 31 December for each year in the rest of this article (Čížek *et al.*, 2005). As $g(X_i)$ is always non-negative, in the long-run we expect S_X will be proportional to the number of storms N. Consequently, the correlation between aggregate severity indices S_X and S_Y of independent hazard variables X and Y for a set of common events is expected to be positive due to both aggregate indices being proportional to N.

exceeded with no damage occurring in coastal and mountainous locations. As a result, use of percentile based thresholds better reflects the climatology of regions. The severity index (SI) used by Klawa and Ulbrich (2003) used the 98th percentile of wind gust speeds alongside the population of an area. This study will use different threshold combinations and only consider meteorological variables for our SIs to focus only on the impact of the hazard. While introducing exposure can improve a SI (Klawa and Ulbrich, 2003), this study chooses to focus on the relationships between hazards.

Few studies have focused on the aggregate severity of European storms. Hunter *et al*. (2015) investigated the relationship between cyclone frequency and mean severity (aggregate severity divided by counts). Using the Blackwell–Girschick equation (Blackwell and Girshick, 1947), the variance of aggregate severity was separated into three components. The term containing the variance of N accounted for 50–80% of the variance of aggregate severity, indicating that event clustering increases variability in aggregate severity. Another variance component was negative in regions of cyclogenesis, but positive in regions of cyclolysis. Although this component was small in magnitude, Hunter *et al*. (2015) concluded assuming independence between frequency and intensity creates large bias in the variance of aggregate risk.

Cyclone clustering is classified as a temporally compounding event (Zscheischler *et al*., 2020). Cyclones in clusters may have greater or smaller risk than a stand-alone event. Events at the end of a cluster may have lower risk as damage has already occurred. Yet an area may be less resilient after the first hazard leading to greater losses from subsequent events. Equation 2 does not account for this temporal compounding as it assumes a constant damage function between events. This study assumes that by raising the damage threshold the frequency of events (and therefore temporal compounding) will be reduced.

Hillier and Dixon (2020) aggregated daily maximum 10m wind gust speed exceeding 20ms^{-1} and total daily precipitation (mm) across seasons to study links between compound events where a time lag exists. An approximate 100% increase of extreme wind in wet years over dry years (upper vs. lower tertiles) was found for the west coasts of the United Kingdom, France and Iberia. One reason for this is only wind or rain being extreme on a daily timescale. As windier storms have higher propagation speeds, they are less able to accumulate precipitation at a given location. Second, persistent environmental conditions over timescales >72h would ensure storms extreme in only one hazard occur, creating the large correlations observed.

Bloomfield *et al*. (2023) investigated the correlation between aggregate wind and flood severity indices for European cyclones over wintertime aggregation periods ranging from 1 to 180 days. The correlations between wind and flood indices were positive but decreased as the length of aggregation period was increased. A peak in correlation occurred between aggregation periods of 40 and 60 days. Bloomfield *et al*. (2023) attributes this to soil saturation, a key flooding precursor, being properly captured by this aggregation period. An accurate flooding severity index should account for such time lag between extreme precipitation and flooding.

Using the definition of ASI in Equation 2, we investigate the questions stated in the Introduction.

Methodology and data

ASI has been calculated for 3s maximum wind gust speeds (S_X) and total precipitation (S_Y) using ERA5 historical reanalysis data (Hersbach *et al*., 2020) at an hourly resolution from 1980 to 2020. Indices were calculated on extratropical cyclone footprints for each footprint grid point on the 0.25° spatial grid. Cyclones were identified, footprints created and ASIs quantified by performing the following operations:

1. Storm tracks in the Northern Hemisphere were identified using the TRACK algorithm (Hodges, 1999) based on hourly values of relative vorticity at 850hPa. Only tracks in the Euro-Atlantic region (30–75°N, 260–40°E) were retained which were separated into calendar years based on their genesis times. The tracks were trimmed within ±36h of the time of maximum gust speed over land to align with the 3-day loss definition for windstorms commonly used in the insurance sector (Mitchell-Wallace *et al*., 2017). Tracks completely over the ocean were not trimmed.

2. Maximum wind and total rainfall footprints were constructed for each track over a Euclidean latitude–longitude distance of 5° around each point on the track. The radius was chosen to be 5° to capture the strongest winds and precipitation (Sinclair *et al*., 2020; Priestley and Catto, 2022) yet is small enough to limit contamination by overlap of different tracks (for more on contamination see Lockwood *et al*., 2022). For each grid point in each footprint, hazard variables were calculated by taking the maximum of the wind gust speeds (X) and the total accumulated precipitation (Y).

3. Annual aggregate severity indices were calculated at each grid point for both hazards using Equation 2 with $k=1$ and threshold combination of choice, (u_X, u_Y). These are summed over all footprints for each calendar year (1 January to 31 December). Sample statistics such as the Pearson product moment correlation between S_X and S_Y (denoted by ρ) were then calculated over the 41 years of the dataset. This step is repeated for a variety of threshold combinations (u_X, u_Y) to obtain more correlation values.

Figure 1 shows example footprints for Storm *Daria*. The 5° radius of influence captures the extreme gust speeds and precipitation. Storm *Daria* had a maximum

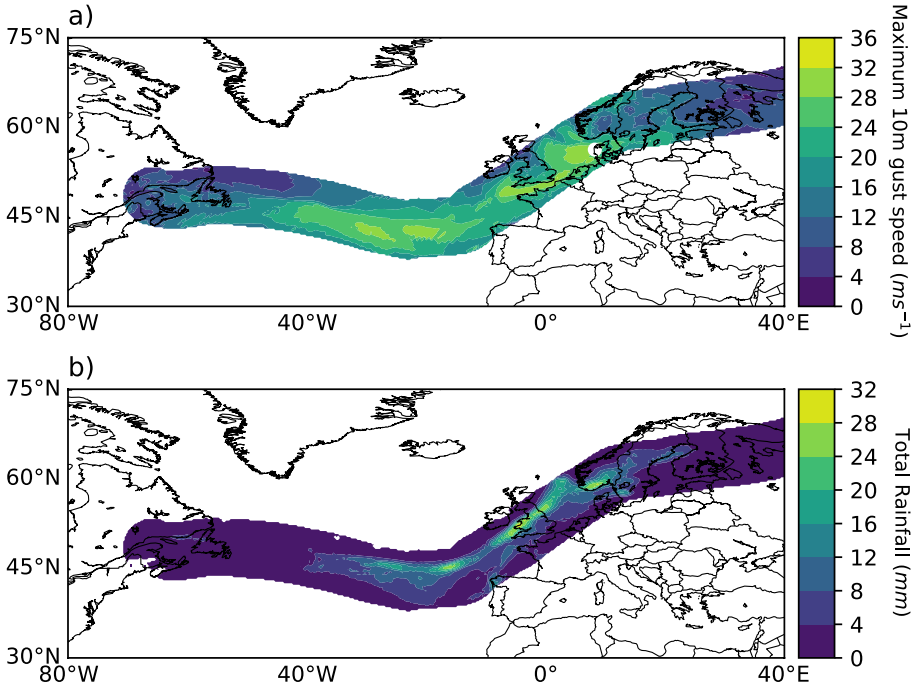

Figure 1. The extracted track for Storm Daria *(24–27 January 1990): (a) maximum 10m wind gust speed, (b) total precipitation. The location of maximum wind gust over land occurred over Denmark (white circle in panel a).*

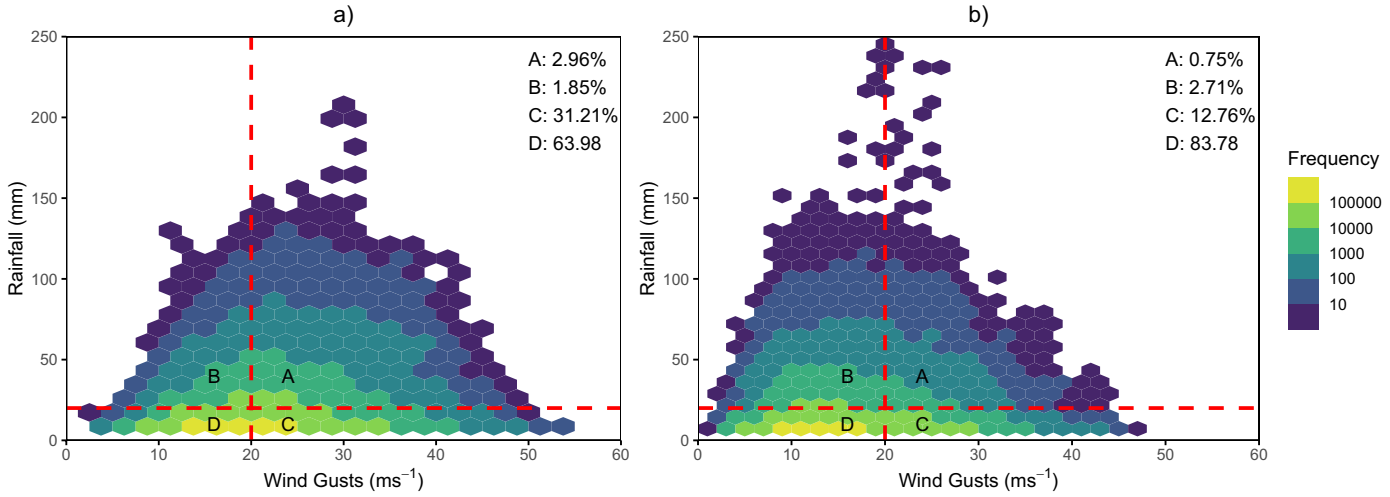

Figure 2. Scatter plots of wind gust speed and rainfall values (X_i, Y_i) over (a) the Azores (37°N, 33°W–45°N, 20.5°W) and (b) France (42.25°N, 4.75°W–51.75°N, 8.5°E). Dashed red lines show thresholds $u_X = 20 ms^{-1}$ and $u_Y = 20 mm$. Percentage of points in each region shown in top right.

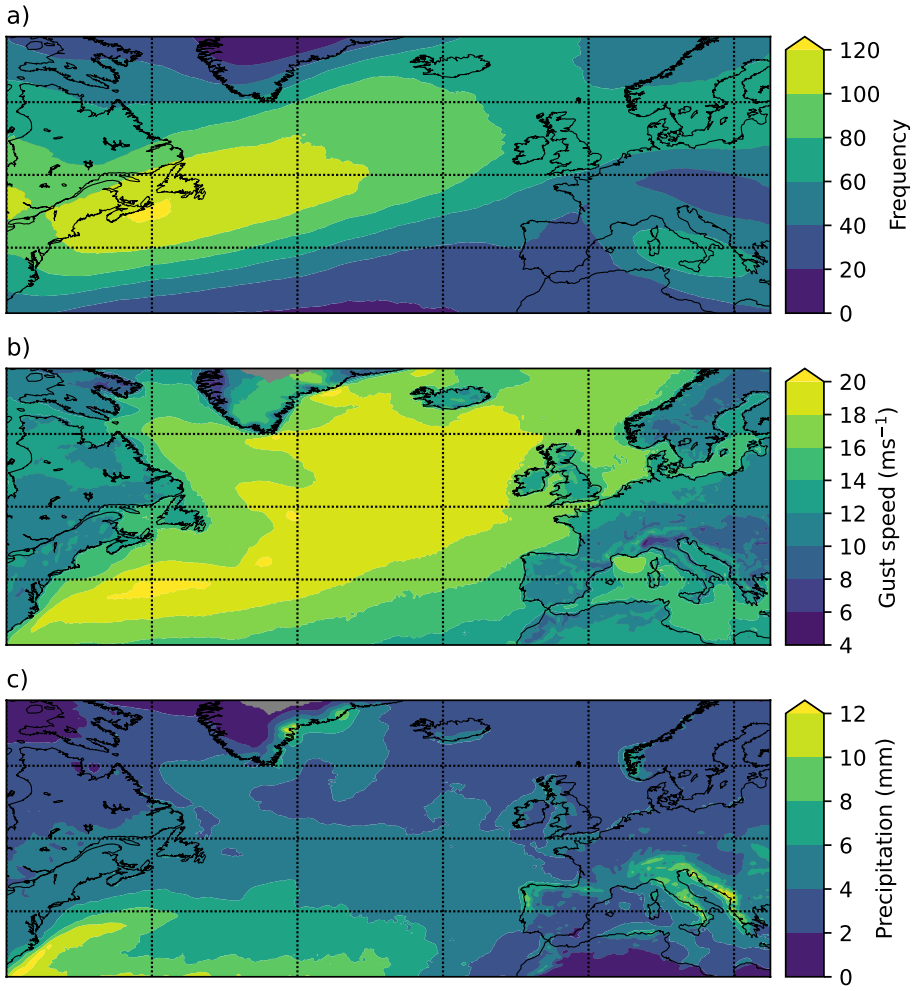

Figure 3. Aggregate summary statistics of footprints for the entire dataset: (a) mean annual counts $\overline{N}$, (b) mean wind severity $\overline{S_X/N}$, and (c) mean precipitation severity $\overline{S_Y/N}$.

land gust speed of 28.7ms^{-1} over Denmark with extreme gust speeds over the United Kingdom, northern France and Denmark. There was severe precipitation and much of this occurred in Wales and central England; the maximum total precipitation was 30mm at a grid box in Wales. The hazards for this storm have different spatial scales, higher precipitation totals occur in a narrower band across the Atlantic and central England while stronger wind gusts are present throughout the storms radius of influence.

Figure 2 shows examples of the wind and precipitation hazard variables over the Azores (Figure 5, Box i) and France (Figure 5, Box ii). These regions were chosen as at higher thresholds correlations between ASIs are mostly positive and negative, respectively (Figure 5). The regions respectively mostly cover the ocean/land and are within the core/exit regions of the North Atlantic storm track. The scatter plot distributions in both regions are bell-shaped but with a shift towards stronger gust speeds in the Azores compared to France. For the thresholds of 20ms^{-1} and 20mm, there are fewer extreme compound events (quadrant A) in France (0.75% of events) than the Azores (2.96%). Whereas the Azores experiences fewer extreme precipitation only events (quadrant B, 1.85%). In both regions, extreme precipitation occurs less often given the most extreme gust speed thresholds (above 30ms^{-1}). At 20ms^{-1} and 20mm extreme events occur more frequently in the Azores (≈64th percentile) than France (≈84th percentile); this is expected as the Azores lies further west and closer to the storm track. One possible reason for this is that the more extreme wind gust speeds are most likely associated with faster moving storms (Hillier and Dixon, 2020) and therefore there is reduced time for precipitation accumulation. The highest rainfall over the Azores occurs at greater gust speeds than for France, as few storms will pass over land before entering the Azores region.

Figure 3 shows aggregate summary statistics for storm counts, maximum gust speed and total precipitation for the entire dataset. The mean counts in Figure 3(a) clearly show the presence of the Atlantic and Mediterranean storm track maxima. The mean wind severity in Figure 3(b) shows a similar yet broader pattern with strong mean wind severity over the central and northern Atlantic Ocean extending towards the west coast of the British Isles. Mean precipitation severity in Figure 3(c) is strongest further south over the Gulf Stream and subtropics and around the Italian and Adriatic coast.

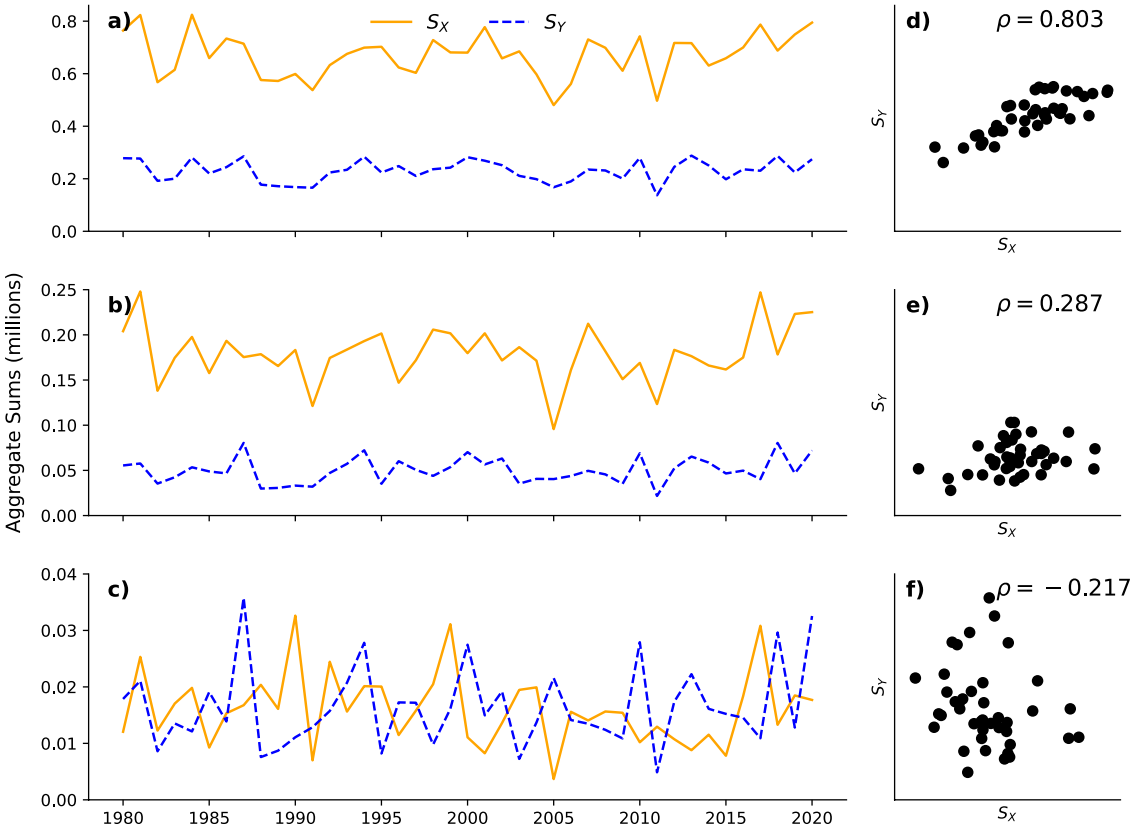

Figure 4. Annual values of total ASI over France from 1980 to 2020 for wind gust speeds (solid yellow line) and precipitation (dashed blue line) and scatter plot of the data. Row is different exceedance threshold pairs (u_x, u_y): (a, d) 0ms^{-1} and 0mm, (b, e) 10ms^{-1} and 10mm, and (c, f) 20ms^{-1} and 20mm.

Correlation of aggregate severity indices

This section explores the relationship between the wind gust speed and precipitation ASIs and how it depends on the choice of thresholds. In addition to spatial maps of correlation at each grid point, sums of ASI over two contrasting regions, France and the Azores, are also compared.

Figure 4 shows ASI summed over all grid points in France at three different choices of thresholds. For thresholds of zero shown in Figure 4(a), the two ASI series exhibit similar peaks and troughs, for example, both ASIs have lower than normal values in 2011. This positive association is to be expected because of the total number of storms having a positive association with both indices. For high values of thresholds shown in Figure 4(c) the ASI series show opposite behaviour with a clear negative association between the two ASI. The ASIs have negative correlation of $\rho = -0.217$, a dramatic reduction from the strong association in panel Figure 4(a). At intermediate threshold values (Figure 4(b)) there is little evidence of either a positive or negative association between the two ASI.

Figure 5 shows the correlation between S_X and S_Y at the same threshold combinations as Figure 4 across the whole of Europe. With thresholds of 0ms^{-1} and 0mm almost the entire region exhibits positive correlation. A small region of negative correlation exists in North Africa, but there is little interest in this relationship as this region has low cyclone activity (see Figure 3(a)). When thresholds are introduced (Figure 5(b)) some negative correlation appears in central Europe and Scandinavia. There is negative correlation in Austria and southern Germany ($\rho < -0.2$) but larger positive correlation in northern Italy ($\rho > 0.7$). These regions are on either side of the lee from the Alps, suggesting an influence of topography on correlation. At the high thresholds, negative correlation is more widespread for all of Europe, however no coherent spatial pattern exists. Correlation is more positive over the ocean and more negative over land. As 20ms^{-1} is

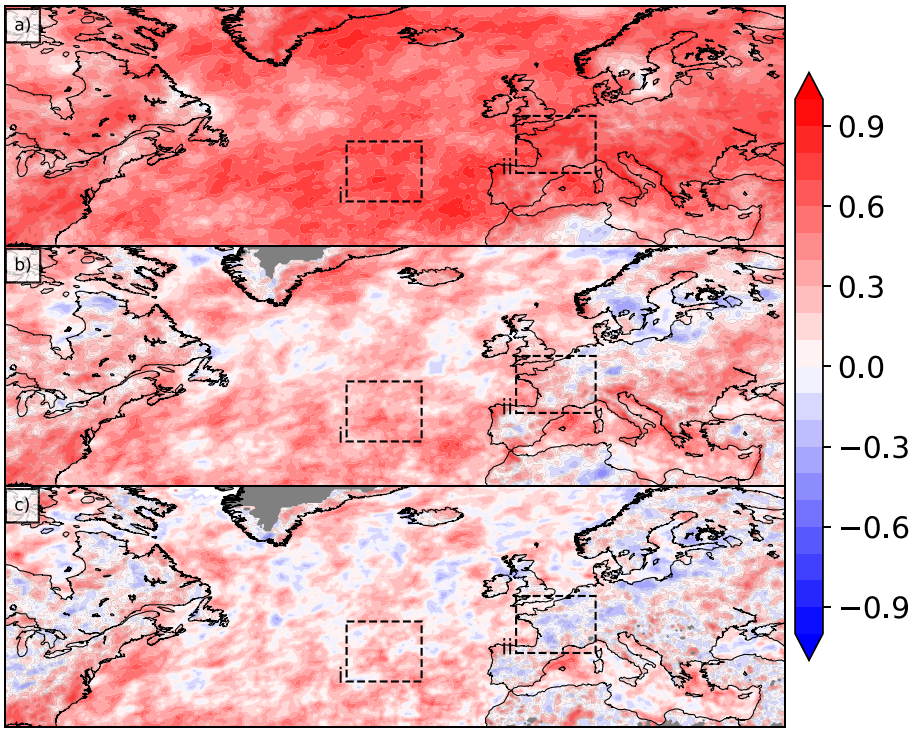

Figure 5. Plot of correlation between aggregate risks S_X and S_Y. Dashed black boxes show regions of interest, the Azores (i) and France (ii). Each panel shows different exceedance thresholds being considered, (a) 0ms^{-1} and 0mm, (b) 10ms^{-1} and 10mm, and (c) 20ms^{-1} and 20mm.

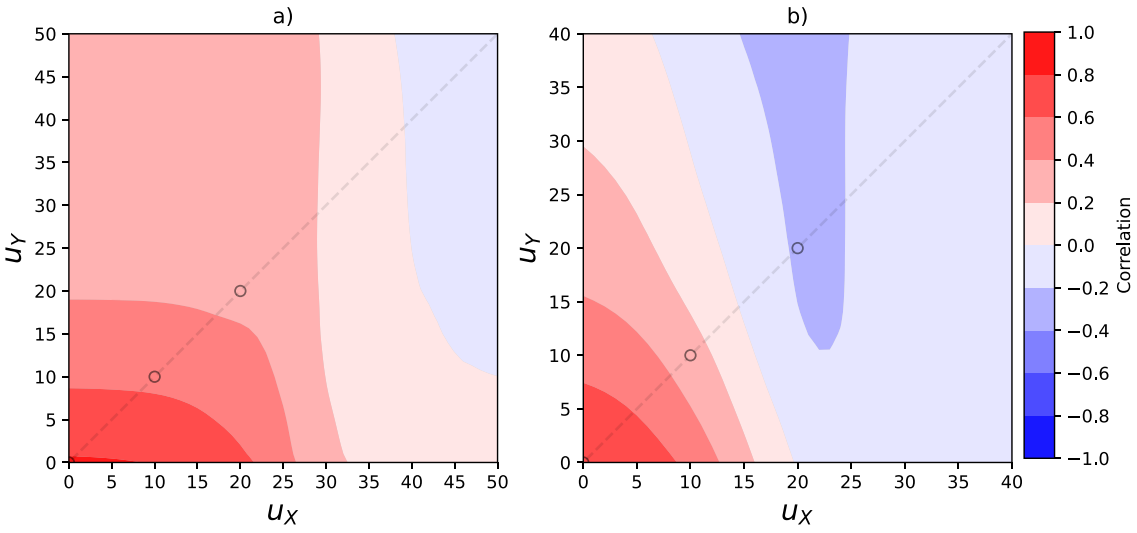

Figure 6. Correlation of S_X and S_Y for different thresholds u_x and u_y: (a) is the Azores region and panel (b) is for France as denoted by Boxes i and ii in Figure 5.

a widely used wind threshold (Klawa and Ulbrich, 2003; Hillier and Dixon, 2020), the existence of negative correlation is important for the consideration of compound hazards. Regional patterns of correlation can be observed in Figure 5(c). The British Isles experiences a north–south divide, with Scotland and parts of North West England experiencing negative correlation, while correlation in the south is positive. Iberia experiences a band of negative correlation across its centre, which may be a result of the fewer events, meaning correlation values are sensitive to extremes. Coastal differences in correlation are also present, northern France and the west coast of Italy have positive correlations while negative correlation exists further inland.

The shift from positive to negative correlation with increasing threshold is also observed when considering only winter extratropical cyclones. When compared to the entire calendar year, the correlation values are mostly closer to one. Stronger positive correlations occur at lower thresholds, while weaker negative values occur at higher thresholds. Correlations closer to one may be explained by a greater frequency and intensity of cyclones during winter. Due to the climatology of European extratropical cyclones, a large portion of yearly losses occur in winter.

Figure 5 shows two regions, the Azores and France. With no thresholds both regions exhibit positive correlation (Figure 5(a)). At highest thresholds, region i (the Azores) has mostly positive correlation, while region ii (France) has negative correlation (Figure 5(c)). As only three combinations of thresholds have been considered Figure 6 explores the structure of correlation for these regions in more depth. The dashed line shows threshold combinations where $u_x = u_y$ with the three threshold combinations considered by Figure 5 in black circles.

Figure 6 shows how the Azores region can have negative correlation at very high thresholds (e.g. $u_x = 45$, $u_y = 35$ where $\rho = -0.0968$). The structure of correlation in the Azores for wind and rain thresholds is different to France. The correlation follows the same contour of $0.2 < \rho < 0.4$ for thresholds $0 < u_x < 30$ and $20 < u_y < 50$. Negative correlation occurs when $u_x > 40$, indicating that the correlation in the Azores is more influenced by the choice of the wind gust threshold. The correlation for France decreases at a more uniform rate with changes in either threshold. Changes are more biased towards wind gusts as a greater change in rainfall threshold is needed to achieve the same change in correlation values. There exists a tongue-like valley of negative correlation between ASIs in France. This occurs with gust speed thresholds of $20 < u_x < 25$ and rainfall thresholds of $10 < u_y < 40$. The highest of the three thresholds considered ($u_x = 20\text{ms}^{-1}$ and $u_y = 20\text{mm}$) lies in this valley. At extreme thresholds fewer data points exist, so correlation is less robust as its more easily affected by extreme values.

This study has used fixed thresholds for the entire study region, whereas other studies have often used percentile based thresholds. Both regions experience near-zero correlation (not shown) when using the 98th percentiles (Azores: $u_{x98} = 31.88\text{ms}^{-1}$ and $u_{y98} = 28.90\text{mm}$, France: $u_{x98} = 27.05\text{ms}^{-1}$ and $u_{y98} = 25.31\text{mm}$). The Azores has a small positive correlation while negative correlation occurs between ASIs over France. The impact of threshold choice on correlation is dependent on the threshold's value relative to individual severities. Although the Azores has higher 98th percentile thresholds than France, it has positive correlation. However the magnitude of values in the Azores are larger, with the Azores experiencing more compound extremes (region A, Figure 2).

Conclusion

This study has examined the relationship between wind gust speed and precipitation annual aggregate severity caused by extratropical cyclones over the Europe-Atlantic sector in the ERA5 reanalysis from 1980 to 2020. Simple aggregate severity indices have been constructed by considering yearly cumulative exceedances above chosen thresholds of wind gust speed maxima and precipitation accumulations for all storms in a year that pass within 5° of each grid point location. These indices can be considered to be simplistic predictors of potential wind- and storm-related aggregate losses.

Strong positive correlation exists at zero thresholds between wind and precipitation aggregate severity over the entire study region. This correlation becomes more negative as thresholds are raised, particularly over Scandinavia and central Europe. High thresholds are commonly used as predictors of insured loss and correlation at these thresholds are negative for wide areas of Western Europe. The transition away from positive correlation is likely a symptom of both aggregate severities at a location having reduced dependence on storm frequency. Hillier and Dixon (2020) proposed this may also be caused by only one ASI being extreme due to lack of events extreme in both severities.

These findings suggest that aggregate wind and flood losses in Europe should not be assumed to be either independent or positively correlated. As often only events above high thresholds cause damage the true correlation between insured losses in Western Europe may be negative, which opens up the possibility of portfolio diversification, that is, it might be possible to partially mitigate flood-related losses using wind-related losses.

This study has some limitations. These include specific design choices such as using a calendar year aggregation period and assuming local exposure to a hazard will result in local damage. For simplicity, only a simple loss function has been considered and future work could explore more realistic formulations of damage functions. For example, this simple loss function for extreme precipitation does not incorporate time lag. This assumes all rivers have small catchments that experience near instantaneous floods.

Different radii of influence could have been considered as 10° has been used in other work (Vitolo *et al*., 2009). Other methods could have been used to prevent footprint contamination, as discussed in Lockwood *et al*. (2022). Not trimming the storm tracks or use of a different tracking algorithm may have yielded different results, as the Hodges (1999) method has longer mean cyclone lifecycles than observations (Bourdin *et al*., 2022).

Correlation values are less robust at higher thresholds as fewer events are considered. This study only uses 41 years of historical reanalysis data so correlation is more affected by extreme values. Future work on correlation between ASIs would benefit from larger datasets. The use of climate model simulations, such as the UNSEEN dataset (Thompson *et al*., 2017), would likely result in robust correlation estimates.

Future yearly storm risk may be compromised from more events extreme in both wind and rain (Bloomfield *et al*., 2024). It is of interest to speculate about what processes are causing the negative correlation and how these may change with global warming. One possibility is that the negative correlation could be related to the speed of transit of storms, which varies from year to year due to changes in westerly flow. In years having a stronger than normal westerly flow, storms will on average move faster and therefore have stronger winds but less time to deposit large amounts of rainfall (i.e. dry windy years). To test such ideas, it would be useful to construct a diagnostic framework (a collective risk model) capable of decomposing the covariance of the ASI into different components to see whether the negative correlation is coming from year-to-year or from within-year correlations between *X* and *Y*.

Author contributions

Toby P. Jones: Methodology; Investigation; Data curation; Writing – original draft; Writing – review & editing; Formal analysis; Visualization; Conceptualization. **David B. Stephenson**: Conceptualization; Methodology; Investigation; Writing – original draft; Writing – review & editing; Supervision. **Matthew D. K. Priestley**: Data curation; Supervision; Writing – review & editing.

Funding statement

TJ is funded by the Engineering and Physical Sciences Research Council [grant no: EP/R513210/1]. MP is funded by the WTW Research Network.

Data availability statement

The data that support the findings of this study are openly available in Copernicus Climate Change Service Climate Data Store at https://doi.org/10.24381/cds.bd0915c6.

References

Bevacqua E, **De Michele C**, **Manning C *et al***. 2021. Guidelines for studying diverse types of compound weather and climate events. *Earth's Future* **9**(11): 1–23. ISSN: 2328-4277. https://doi.org/10.1029/2021EF002340

Blackwell D, **Girshick MA**. 1947. A lower bound for the variance of some unbiased sequential estimates. *Ann. Math. Stat.* **18**(2): 277–280. https://doi.org/10.1214/aoms/1177730444

Bloomfield HC, **Bates P**, **Shaffrey LC** *et al*. 2024. Synoptic conditions conducive for compound wind-flood events in Great Britain in present and future climates. *Environ. Res. Lett.* **19**(2). ISSN: 1748-9326. https://doi.org/10.1088/1748-9326/ad1cb7

Bloomfield HC, **Hillier J**, **Griffin A *et al***. 2023. Co-occurring wintertime flooding and extreme wind over Europe, from daily to seasonal timescales. *Weather Clim. Extrem.* **39**. https://doi.org/10.1016/j.wace.2023.100550

Bourdin S, **Fromang S**, **Dulac W *et al***. 2022. Intercomparison of four algorithms for detecting tropical cyclones using ERA5. *Geosci. Model Dev.* **15**(17): 6759–6786. https://doi.org/10.5194/gmd-15-6759-2022

Catto JL, **Dowdy A**. 2021. Understanding compound hazards from a weather system perspective. *Weather Clim. Extrem.* **32**: 100313. ISSN: 2212-0947. https://doi.org/10.1016/j.wace.2021.100313

Čížek P, **Weron R**, **Härdle W**. 2005. Statistical Tools for Finance and Insurance, Volume 1. Springer Berlin: Heidelberg, pp 407–426. https://doi.org/10.1007/b139025.

Hersbach H, **Bell B**, **Berrisford P *et al***. 2020. The ERA5 global reanalysis. *Q. J. R. Meteorol. Soc.* **146**(730): 1999–2049. https://doi.org/10.1002/qj.3803

Hillier JK, **Dixon RS**. 2020. Seasonal impact-based mapping of compound hazards. *Environ. Res. Lett.* **15**(11): 114013. https://doi.org/10.1088/1748-9326/abbc3d

Hodges KI. 1999. Adaptive constraints for feature tracking. *Mon. Weather Rev.* **127**(6): 1362–1373. https://doi.org/10.1175/1520-0493(1999)127<1362:acfft>2.0.co;2

Hunter A, **Stephenson DB**, **Economou T *et al***. 2015. New perspectives on the collective risk of extratropical cyclones. *Q. J. R. Meteorol. Soc.* **142**(694): 243–256. https://doi.org/10.1002/qj.2649

Kaas R, **Goovaerts M**, **Dhaene J *et al***. 2008. Modern Actuarial Risk Theory, Volume 2. chapter = 3. Springer Berlin: Heidelberg. https://doi.org/10.1007/978-3-540-70 998-5.

Klawa M, **Ulbrich U**. 2003. A model for the estimation of storm losses and the identification of severe winter storms in Germany. *Nat. Hazards Earth Syst. Sci.* **3**: 725–732. https://doi.org/10.5194/nhess-3-725-2003

Lockwood JF, **Guentchev GS**, **Alabaster A *et al***. 2022. Using high-resolution global climate models from the PRIMAVERA project to create a European winter windstorm event set. *Nat. Hazards Earth Syst. Sci.* **22**(11): 3585–3606. https://doi.org/10.5194/nhess-22-3585-2022

Mailier PJ, **Stephenson DB**, **Ferro CAT** *et al*. 2006. Serial clustering cyclones. *Mon. Weather Rev.* **134**(8): 2224–2240. https://doi.org/10.1175/MWR3160.1

Martius O, **Pfahl S**, **Chevalier C**. 2016. A global quantification of compound precipitation and wind extremes. *Geophys. Res. Lett.* **43**(14): 7709–7717. ISSN: 1944-8007. https://doi.org/10.1002/2016GL070017

Mitchell-Wallace K, **Foote M**, **Hillier J *et al***. 2017. Natural Catastrophe Risk Management and Modelling. Hoboken: John Wiley & Sons, Ltd. https://doi.org/10.1002/9781118906057.

Owen LE, **Catto JL**, **Stephenson DB *et al***. 2021. Compound precipitation and wind extremes over Europe and their relationship to extratropical cyclones. *Weather Clim. Extrem.* **33**. https://doi.org/10.1016/j.wace.2021.100342

Priestley MDK, **Catto JL**. 2022. Improved representation of extratropical cyclone structure in HighResMIP models. *Geophys. Res. Lett.* **49**(5). ISSN: 1944-8007. https://doi.org/10.1029/2021gl096708

Raveh-Rubin S, **Wernli H**. 2015. Large-scale wind and precipitation extremes in the Mediterranean: a climatological analysis for 1979–2012. *Q. J. R. Meteorol. Soc.* **141**(691): 2404–2417. https://doi.org/10.1002/qj.2531

Sinclair VA, **Rantanen M**, **Haapanala P *et al***. 2020. The characteristics and structure of extra-tropical cyclones in a warmer climate. *Weather Clim. Dyn.* **1**(1): 1–25. ISSN: 2698-4016. https://doi.org/10.5194/wcd-1-1-2020

Thompson V, **Dunstone NJ**, **Scaife AA** *et al*. 2017. High risk of unprecedented UK rainfall in the current climate. *Nat. Commun.* **8**(1). ISSN: 2041-1723. https://doi.org/10.1038/s41467-017-00275-3

Ulbrich U, **Fink AH**, **Klawa M *et al***. 2001. Three extreme storms over Europe in December 1999. *Weather* **56**(3): 70–80. ISSN: 1477-8696. https://doi.org/10.1002/j.1477-8696.2001.tb06540.x

Vitolo R, **Stephenson DB**, **Cook IM *et al***. 2009. Serial clustering of intense European storms. *Meteorol. Z.* **18**(4): 411–424. https://doi.org/10.1127/0941-2948/2009/0393

Zscheischler J, **Martius O**, **Westra S *et al***. 2020. A typology of compound weather and climate events. *Nat. Rev. Earth Environ.* **1**(7): 333–347. https://doi.org/10.1038/s43017-020-0060-z

Correspondence to: T. P. Jones
tpj201@exeter.ac.uk

doi: 10.1002/wea.4573